A Double Homotopy Approach for Decentralized $\mathcal{H}_\infty$ Control of Civil Structures

Chunxu Qu [1,2], Linsheng Huo [1,*,†] , Hongnan Li [1], Yang Wang [2]

[1] Faculty of Infrastructure Engineering, Dalian University of Technology, Dalian 116024, China

[2] School of Civil and Environmental Engineering, Georgia Institute of Technology, Atlanta, GA 30332, USA

ABSTRACT

This paper presents a decentralized $\mathcal{H}_\infty$ controller design for the vibration control of civil structures. The formulation through double homotopy is proposed in discrete time domain and considers feedback time delay. It is well known that through bounded real lemma, $\mathcal{H}_\infty$ controller design can be transformed to an optimization problem with bilinear matrix inequality (BMI) constraints. To obtain a decentralized $\mathcal{H}_\infty$ controller constrained by special block-diagonal patterns on controller matrices, there is generally no off-the-shelf package or numerical algorithm to solve the BMI problem. This paper proposes a double homotopy method to solve the BMI problem in discrete time domain. The method approximates the BMI problem to a series of linear matrix inequality (LMI) problems along two homotopic paths, and gradually deforms a centralized controller to a decentralized controller. The proposed method is first studied numerically with a six-story building example, and then validated experimentally through shaking table tests of a two-story frame with active mass dampers.

KEY WORDS: structural control; decentralized control; bilinear matrix inequality; double homotopy; time delay; civil structures

INTRODUCTION

Excessive dynamic excitations upon civil structures, such as earthquakes and wind load, can cause significant structural vibrations and result in damage to structural components. Structural control is a promising method to protect structures from damage. A great amount of research efforts have been devoted to active or semi-active feedback control [1-4]. Such a feedback control system contains sensors, controllers, and control devices. Sensors measure structural vibration data caused by external excitations. Sensor data is then transmitted to controllers, which make control decisions accordingly, and command the control devices to generate desired forces for vibration reduction. Traditional structural feedback control adopts centralized control schemes, where a centralized controller requires data from all sensors in the structure and delivers

* Correspondence to: Linsheng Huo, of Infrastructure Engineering, Dalian University of Technology, Dalian 116024, China.
†E-mail: lshuo@dlut.edu.cn

command to all structural control devices. Particularly for large-scale civil structures, a centralized feedback control scheme places high requirements on real-time communication range and data transmission rate, which result in economical and technical difficulties in practical implementation.

As an alternative, decentralized control architectures can be employed. A decentralized architecture allows control decisions to be made using sensor data only in the neighborhood of a control device [5, 6]. As a result, communication range and data transmission rate are reduced. Feedback latency of the control system is also shortened. Decentralized control has been investigated in applications such as power transmission networks, economic systems, and space systems [7]. However, decentralized structural control has only been studied in recent years. For example, Lynch and Law [8] discussed modified decentralized LQR control and decentralized market-based control for large-scale civil structures. Xu *et al.* [9] proposed a decentralized tendon control algorithm for a cable-stayed bridge with neural networks. Swartz and Lynch [10] employed the redundant Kalman state-estimators for distributed structural control system. Rofooei and S.Monajemi-Nezhad [11] investigated decentralized schemes in which instantaneous optimal control schemes are used with different control feedbacks. Lu *et al.* [12] described the fully decentralized sliding mode control algorithms, which make control decision based on the stroke velocity and displacement measured on a control device. Ma *et al.* [13] studied decentralized robust control of building structures by treating the interconnections between adjacent subsystems as bounded disturbances. Loh and Chang [14] compared four groups of centralized/decentralized control algorithms, including fully centralized, fully decentralized, half centralized, and partially decentralized control. More recently, feedback time delay, such as due to communication and computing, is taken into consideration for decentralized dynamic output feedback control [15, 16]. In general, the more sensor data each control device requires, the larger the time delay is. Time delay can be measured and calculated as part of the system performance, such as for a wireless feedback control system [17]. Considering feedback time delay in the control formulation, this paper presented a new $\mathcal{H}_\infty$ structural control design for decentralized dynamic output feedback control in discrete time domain.

Bounded real lemma [18] can be used to provide an effective method to calculate the $\mathcal{H}_\infty$ controller matrices. The controller matrices are constrained by bilinear matrix inequality (BMI) [19]. When no special patterns are required on controller matrices, the matrices can be solved by projection lemma [18]. On the other hand, when a decentralized controller is desired, block-diagonal patterns are required on the controller matrices. The pattern requirement makes the decentralized controller design a non-convex and NP-hard problem. There is no general off-the-shelf package or numerical algorithm for this decentralized control problem. For example, when the PENNON (PENalty methods for NONlinear optimization) package was attempted for solving non-convex optimization problems, it was realized the idea was not yet mature and further tuning was needed [20]. Wang [16] modified a continuous-time homotopy method for discrete-time decentralized $\mathcal{H}_\infty$ controller design with feedback time delay. Along the homotopy path, the centralized controller is gradually transformed to a decentralized controller. Only linear matrix inequality (LMI) problems are involved at each homotopy step, which avoids directly solving the BMI problem. As an alternative method to deal

with BMI constraints, Mehendale and Grigoriadis [21] proposed a double homotopy approach for decentralized $\mathcal{H}_\infty$ control in continuous time domain without time delay. This paper modifies the double homotopy method for decentralized control design in discrete time domain and considering feedback time delay. Along one homotopy path, the centralized controller is slowly deformed to a decentralized controller. Along the other homotopy path, the solution to the BMI problem is gradually improved by local linearization. In a previous discrete-time homotopy approach described by Wang [16], at every homotopy step, the controller matrix or the Lyapunov matrix is held constant in turn while solving the other. In comparison, the double homotopy approach updates the controller matrix and Lyapunov matrix simultaneously by local linearization to the original BMI problem. In addition, minimization of closed-loop $\mathcal{H}_\infty$ norm is performed at every double homotopy step, in order to avoid resulting in a decentralized controller with a very large $\mathcal{H}_\infty$ norm. Both numerical simulations and laboratory experiments were performed to validate the proposed discrete-time decentralized control design through double homotopy.

The paper first introduces the problem formulation for decentralized structural control considering time delay. The decentralized $\mathcal{H}_\infty$ control through double homotopy transformation in discrete time domain is then presented. A six-story numerical example is described to illustrate the decentralized $\mathcal{H}_\infty$ control performance. Finally, the paper describes experimental validation through shaking table tests of a two-story frame with active mass dampers.

PROBLEM FORMULATION

Consider a second-order differential equation describing the dynamics of an *n* degree-of-freedom (DOF) shear-frame structure:

$$M\ddot{q} + C\dot{q} + Kq = T_{w1}w_1 + T_u u \tag{1}$$

where $M, C, K \in \Re^{n\times n}$ are the mass, damping, and stiffness matrices, respectively; $w_1 \in \Re^{n_{w1}\times 1}$ is the external excitation vector; $u \in \Re^{n_u \times 1}$ is the control force vector; T_{w1} and T_u are the location matrices for excitation w_1 and control force u, respectively. When the excitation w_1 is the unidirectional earthquake acceleration $\ddot{q}_g$, the excitation location matrix can be found as $T_{w1} = -M\{1\}_{n\times 1}$. The relative displacement vector $q \in \Re^{n\times 1}$ is defined as:

$$q = \begin{bmatrix} q_1 & q_2 & \cdots & q_n \end{bmatrix}^{\mathrm{T}} \tag{2}$$

where q_i denotes the relative displacement (with respect to the ground) of the *i*-th floor. To suppress excessive structural vibration excited by w_1, appropriate control force u should be imposed on the structure. In an optimal feedback control system, a controller is pre-designed. During system operation, according to available sensor measurements, the

controller decides in real time the optimal control force to be applied by each control device. In practice, sensor measurements are usually contaminated by noises. In addition, transmission of measurement data to controller, as well as controller computation, causes time delay in the feedback loop.

To describe both sensor noise and feedback time delay, the structural system in Eq.(1) can be re-written into state space representation and transformed from continuous time domain to discrete time domain. The structural system is then concatenated with an auxiliary LTI (linear time-invariant) system describing the sensor noise and time delay, as shown in Figure 1. After the concatenation, the discrete-time open-loop system can be formulated as [16]:

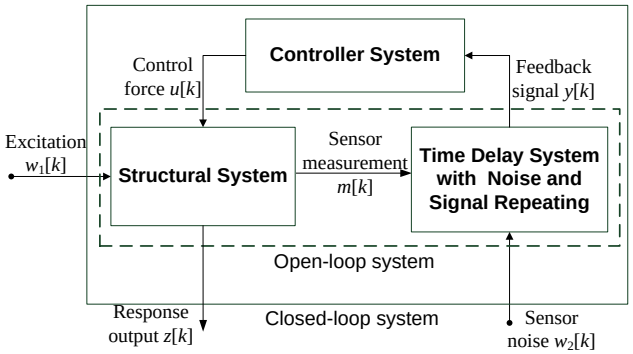

Figure 1. Diagram of the Structural Control System

$$\begin{cases} x[k+1] = Ax[k] + B_1 w[k] + B_2 u[k] \\ z[k] = C_1 x[k] + D_{11} w[k] + D_{12} u[k] \\ y[k] = C_2 x[k] + D_{21} w[k] \end{cases} \tag{3}$$

where $w = [w_1 \quad w_2]^{\mathrm{T}} \in \Re^{n_w \times 1}$ contains excitation $w_1 \in \Re^{n_{w1} \times 1}$ and sensor noise $w_2 \in \Re^{n_{w2} \times 1}$, where $n_w = n_{w1} + n_{w2}$; $y \in \Re^{n_y \times 1}$ contains the time-delayed and noisy sensor signals; $u \in \Re^{n_u \times 1}$ is the same control force vector as in Eq.(1). The open-loop system state vector, $x \in \Re^{n_{OL} \times 1}$, contains structural system state vector, $x_S \in \Re^{2n \times 1}$, and time-delay system state vector, $x_{TD} \in \Re^{n_{TD} \times 1}$. For the lumped mass shear-frame model with n stories, q_i and $\dot{q}_i$ denote relative displacement and relative velocity, respectively (with respect to the ground), of the i-th floor (i = 1,…, n). To facilitate decentralized feedback formulation, structural state vector x_S is organized by grouping relative displacement and velocity at each floor:

$$x_S = [q_1 \quad \dot{q}_1 \quad q_2 \quad \dot{q}_2 \quad \ldots \quad q_n \quad \dot{q}_n]^{\mathrm{T}} \tag{4}$$

The matrices A, B_1, B_2 in Eq. (3) are the state transition, the excitation influence, and the control influence matrices. Vector $z \in \Re^{n_z \times 1}$ is the open loop system response that

the system aims to control, and $y \in \Re^{n_y \times 1}$ is the sensor measurement with time delay and noise. To complete a feedback loop, vector y also serves as the input to the controller system to be designed, which is described as:

$$\begin{cases} x_G[k+1] = A_G x_G[k] + B_G y[k] \\ u[k] = C_G x_G[k] + D_G y[k] \end{cases} \tag{5}$$

where $x_G \in \Re^{n_G \times 1}$ is the controller state vector; A_G, B_G, C_G, D_G are constant matrices of the LTI dynamic controller and are to be determined through an optimal control design.

DECENTRALIZED CONTROLLER DESIGN IN DISCRETE TIME THROUGH DOUBLE HOMOTOPY APPROACH

Decentralized Controller Design

For decentralized controller design, the decentralization is represented through block-diagonal patterns in the controller matrices:

$$\begin{aligned} A_G &= \text{diag}\left(A_{G_1}, A_{G_2}, \cdots A_{G_N}\right) \\ B_G &= \text{diag}\left(B_{G_1}, B_{G_2}, \cdots B_{G_N}\right) \\ C_G &= \text{diag}\left(C_{G_1}, C_{G_2}, \cdots C_{G_N}\right) \\ D_G &= \text{diag}\left(D_{G_1}, D_{G_2}, \cdots D_{G_N}\right) \end{aligned} \tag{6}$$

With the block-diagonal patterns, the controller system in Eq. (5) is equivalent to multiple sub-controllers that are independent from each other. Every sub-controller needs only part of sensor measurement data as input and determines only part of the control forces as output:

$$\begin{cases} x_{G_1}[k+1] = A_{G_1} x_{G_1}[k] + B_{G_1} y_1[k] \\ u_1[k] = C_{G_1} x_{G_1}[k] + D_{G_1} y_1[k] \end{cases}$$

$$\cdots,$$

$$\begin{cases} x_{G_i}[k+1] = A_{G_i} x_{G_i}[k] + B_{G_i} y_i[k] \\ u_i[k] = C_{G_i} x_{G_i}[k] + D_{G_i} y_i[k] \end{cases} \tag{7}$$

$$\cdots,$$

$$\begin{cases} x_{G_N}[k+1] = A_{G_N} x_{G_N}[k] + B_{G_N} y_N[k] \\ u_N[k] = C_{G_N} x_{G_N}[k] + D_{G_N} y_N[k] \end{cases}$$

where $A_{G_i}, B_{G_i}, C_{G_i}, D_{G_i}$ are matrices of the i-th sub-controller, i=1…N); y_i is the sensor measurement data required by the i-th sub-controller; u_i is the control force determined

by the *i*-th sub-controller. As a result, the overall sensor measurement and control force vectors are partitioned by sub-controllers:

$$y = \begin{bmatrix} y_1 & \cdots & y_i & \cdots & y_N \end{bmatrix}^{\mathrm{T}} \tag{8a}$$

$$u = \begin{bmatrix} u_1 & \cdots & u_i & \cdots & u_N \end{bmatrix}^{\mathrm{T}} \tag{8b}$$

For convenience in later derivation, the following notations should be defined first based on parametric matrices of the open-loop system in Eq.(3):

$$\left[\begin{array}{c|c|c} \tilde{A} & \tilde{B}_1 & \tilde{B}_2 \\ \hline \tilde{C}_1 & \tilde{D}_{11} & \tilde{D}_{12} \\ \hline \tilde{C}_2 & \tilde{D}_{21} & \end{array}\right] = \left[\begin{array}{cc|c|cc} A & 0 & B_1 & 0 & B_2 \\ 0 & 0 & 0 & I_{n_G} & 0 \\ \hline C_1 & 0 & D_{11} & 0 & D_{12} \\ \hline 0 & I_{n_G} & 0 & & \\ C_2 & 0 & D_{21} & & \end{array}\right] \tag{9}$$

where n_G is the order of decentralized controller. Combining the open-loop system and the controller system in Eq. (5), the closed-loop system is formulated as:

$$\begin{cases} x_{CL}[k+1] = A_{CL} x_{CL}[k] + B_{CL} w[k] \\ z[k] = C_{CL} x_{CL}[k] + D_{CL} w[k] \end{cases} \tag{10a}$$

$$A_{CL} = \tilde{A} + \tilde{B}_2 G \tilde{C}_2 \tag{10b}$$

$$B_{CL} = \tilde{B}_1 + \tilde{B}_2 G \tilde{D}_{21} \tag{10c}$$

$$C_{CL} = \tilde{C}_1 + \tilde{D}_{12} G \tilde{C}_2 \tag{10d}$$

$$D_{CL} = \tilde{D}_{11} + \tilde{D}_{12} G \tilde{D}_{21} \tag{10e}$$

where x_{CL} is the state vector of the closed-loop system; G is the overall controller matrix that contains all four parametric matrices in the controller system:

$$G = \begin{bmatrix} A_G & B_G \\ C_G & D_G \end{bmatrix} \tag{11}$$

An $\mathcal{H}_\infty$ controller design aims to determine a proper controller matrix G so that $\mathcal{H}_\infty$ norm of the closed-loop system is minimized. As a result, dynamic response of the structural system is reduced. According to bounded real lemma in discrete time, an $\mathcal{H}_\infty$ controller can be designed to make the closed-loop system stable and its $\mathcal{H}_\infty$ norm smaller than a given scalar γ, if and only if, there exists a symmetric positive definite matrix $P > 0$ such that the following matrix inequality holds:

$$\begin{bmatrix} -P & PA_{CL} & PB_{CL} & 0 \\ * & -P & 0 & C_{CL}^{\mathrm{T}} \\ * & * & -\gamma I & D_{CL}^{\mathrm{T}} \\ * & * & * & -\gamma I \end{bmatrix} < 0 \tag{12}$$

where $(*)$ denotes the terms induced by symmetry. Substituting Eq.(10b) - (10e) into Eq.(12), the matrix inequality now contains the controller matrix *G* and other constant parametric matrices defined in Eq. (9):

$$\begin{bmatrix} -P & P\left(\tilde{A}+\tilde{B}_2 G\tilde{C}_2\right) & P\left(\tilde{B}_1+\tilde{B}_2 G\tilde{D}_{21}\right) & 0 \\ * & -P & 0 & \left(\tilde{C}_1+\tilde{D}_{12} G\tilde{C}_2\right)^{\mathrm{T}} \\ * & * & -\gamma I & \left(\tilde{D}_{11}+\tilde{D}_{12} G\tilde{D}_{21}\right)^{\mathrm{T}} \\ * & * & * & -\gamma I \end{bmatrix} < 0 \tag{13}$$

Linear Matrix Inequality and Bilinear Matrix Inequality

A linear matrix inequality (LMI) has the form as the following [19]:

$$F(x) = F_0 + \sum_{i=1}^{m} x_i F_i > 0 \tag{14}$$

where $x \in \Re^m$ is the vector variable and the symmetric matrices $F_i = F_i^{\mathrm{T}} \in \Re^{n\times n}$, i = 0,…,*m*, are given. The inequality symbol in Eq.(14) means that $F(x)$ is positive definite. An important property of LMI is that the set $\{x \mid F(x) > 0\}$ is convex, which can serve as constraint of a convex optimization problem. On the other hand, the bilinear matrix inequality (BMI) is of the form:

$$F(x,y) = F_0 + \sum_{i=1}^{m} x_i F_i + \sum_{j=1}^{n} y_j G_j + \sum_{i=1}^{m}\sum_{j=1}^{n} x_i y_j H_{ij} > 0 \tag{15}$$

where G_j and H_{ij} are symmetric matrices, and $x \in \Re^m$ and $y \in \Re^n$ are vector variables. A BMI is an LMI in *x* for fixed *y*, or an LMI in *y* for fixed *x*. However, the BMI constraint doesn't provide a convex set on *x* and *y* simultaneously.

Double Homotopy Approach

Eq. (13) has terms of matrix product that involves both unknown variables *P* and *G*, which results in a bilinear matrix inequality (BMI). When there is no special pattern requirement on *G*, such as in a traditional centralized controller design, the BMI problem can be solved by projection lemma [18]. However, with a block-diagonal pattern constraint to the matrix variable *G*, as required by a decentralized design, the problem

becomes NP-hard. There is no general off-the-shelf numerical package or algorithm for such a non-convex decentralized control problem. For example, algorithm in the PENNON package is modified for finding local minima or stationary points in a nonconvex problem, but the idea is found to be not yet mature and needs further tuning [20]. More recently, Mehendale and Grigoriadis [21] proposed a heuristic double homotopy algorithm to solve the decentralized $\mathcal{H}_\infty$ controller in continuous time domain. In this paper, the double homotopy concept is adopted to design a decentralized $\mathcal{H}_\infty$ controller in discrete time domain.

To obtain a decentralized controller through numerical iteration, the double homotopy algorithm approximates BMI to easily solvable LMIs, and then gradually changes the diagonal-block entries of a centralized controller. At the same time, the off-diagonal-block entries are transformed to zero along the homotopy steps. At the first step (step number k = 0), the initial G and P are set to the same as centralized controller matrix G_C and co-existing P_C:

$$G_0 = G_C = G_{C,diag} + G_{C,off} \tag{16a}$$

$$P_0 = P_C \tag{16b}$$

where $G_{C,diag}$ represents the block diagonal part of G_C that has the same sparsity pattern as the desired decentralized controller matrix; $G_{C,off}$ denotes the off-diagonal blocks such that Eq. (16a) is satisfied. At the k-th homotopy step (k = 1, 2, …, K), P_k and G_k are described as the following:

$$\lambda = 1/K \tag{17a}$$

$$G_k = G_{k-1} - \lambda G_{C,off} + \Delta G_k \tag{17b}$$

$$P_k = P_{k-1} + \Delta P_k \tag{17c}$$

where K is the total number of steps; the increment ΔG_k has the same structure as $G_{C,diag}$; the increment ΔP_k is symmetric. When the step k changes from 1 to K, the off-diagonal block entries of the controller G_k are gradually transformed to zero, and the diagonal block entries are changed by the increments ΔG_k. When ΔG_k and ΔP_k are small enough, their products can be neglected. Therefore, the bilinear entries in Eq. (13) can be approximately linearized as the following:

$$\begin{aligned}
&P_k\left(\tilde{A}+\tilde{B}_2 G_k \tilde{C}_2\right)\\
&=\left(P_{k-1}+\Delta P_k\right)\left[\tilde{A}+\tilde{B}_2\left(G_{k-1}+\Delta G_k-\lambda G_{C,off}\right)\tilde{C}_2\right]\\
&=P_{k-1}\left[\tilde{A}+\tilde{B}_2\left(G_{k-1}-\lambda G_{C,off}\right)\tilde{C}_2\right]+P_{k-1}\tilde{B}_2\Delta G_k\tilde{C}_2+\Delta P_k\left[\tilde{A}+\tilde{B}_2\left(G_{k-1}-\lambda G_{C,off}\right)\tilde{C}_2\right]+\Delta P_k\tilde{B}_2\Delta G_k\tilde{C}_2\\
&\approx P_{k-1}\bar{A}+P_{k-1}\tilde{B}_2\Delta G_k\tilde{C}_2+\Delta P_k\bar{A}
\end{aligned} \tag{18a}$$

$$
\begin{aligned}
&P_k\left(\tilde{B}_1+\tilde{B}_2G_k\tilde{D}_{21}\right)\\
&=\left(P_{k\text{-}1}+\Delta P_k\right)\left[\tilde{B}_1+\tilde{B}_2\left(G_{k\text{-}1}+\Delta G_k-\lambda G_{C,off}\right)\tilde{D}_{21}\right]\\
&=P_{k\text{-}1}\left[\tilde{B}_1+\tilde{B}_2\left(G_{k\text{-}1}-\lambda G_{C,off}\right)\tilde{D}_{21}\right]+P_{k\text{-}1}\tilde{B}_2\Delta G_k\tilde{D}_{21}+\Delta P_k\left[\tilde{B}_1+\tilde{B}_2\left(G_{k\text{-}1}-\lambda G_{C,off}\right)\tilde{D}_{21}\right]+\Delta P_k\tilde{B}_2\Delta G_k\tilde{D}_{21}\\
&\approx P_{k-1}\bar{B}+P_{k-1}\tilde{B}_2\Delta G_k\tilde{D}_{21}+\Delta P_k\bar{B}
\end{aligned}
\tag{18b}
$$

As a result, the BMI problem is converted to an LMI problem where there is no matrix product simultaneously involving ΔG_k and ΔP_k. Substituting G_k in Eq.(17b) into other entries in Eq.(13), the following equation can be derived:

$$
\begin{aligned}
\tilde{C}_1+\tilde{D}_{12}G_k\tilde{C}_2&=\tilde{C}_1+\tilde{D}_{12}\left(G_{k\text{-}1}+\Delta G_k-\lambda G_{C,off}\right)\tilde{C}_2\\
&=\tilde{C}_1+\tilde{D}_{12}\left(G_{k\text{-}1}-\lambda G_{C,off}\right)\tilde{C}_2+\tilde{D}_{12}\Delta G_k\tilde{C}_2 \qquad (19a)\\
&=\bar{C}+\tilde{D}_{12}\Delta G_k\tilde{C}_2\\
\tilde{D}_{11}+\tilde{D}_{12}G_k\tilde{D}_{21}&=\tilde{D}_{11}+\tilde{D}_{12}\left(G_{k\text{-}1}+\Delta G_k-\lambda G_{C,off}\right)\tilde{D}_{21}\\
&=\tilde{D}_{11}+\tilde{D}_{12}\left(G_{k\text{-}1}-\lambda G_{C,off}\right)\tilde{D}_{21}+\tilde{D}_{12}\Delta G_k\tilde{D}_{21} \qquad (19b)\\
&=\bar{D}+\tilde{D}_{12}\Delta G_k\tilde{D}_{21}
\end{aligned}
$$

where

$$\bar{A}=\tilde{A}+\tilde{B}_2\left(G_{k\text{-}1}-\lambda G_{C,off}\right)\tilde{C}_2 \tag{20a}$$

$$\bar{B}=\tilde{B}_1+\tilde{B}_2\left(G_{k\text{-}1}-\lambda G_{C,off}\right)\tilde{D}_{21} \tag{20b}$$

$$\bar{C}=\tilde{C}_1+\tilde{D}_{12}\left(G_{k\text{-}1}-\lambda G_{C,off}\right)\tilde{C}_2 \tag{20c}$$

$$\bar{D}=\tilde{D}_{11}+\tilde{D}_{12}\left(G_{k\text{-}1}-\lambda G_{C,off}\right)\tilde{D}_{21} \tag{20d}$$

Finally, the LMI after linearizing BMI in Eq. (13) can be re-written with variables ΔG_k and ΔP_k:

$$
V\left(\Delta G_k,\Delta P_k\right)=
\begin{bmatrix}
P_{k-1}+\Delta P_k & P_{k-1}\bar{A}+P_{k-1}\tilde{B}_2\Delta G_k\tilde{C}_2+\Delta P_k\bar{A} & P_{k-1}\bar{B}+P_{k-1}\tilde{B}_2\Delta G_k\tilde{D}_{21}+\Delta P_k\bar{B} & 0\\
* & P_{k-1}+\Delta P_k & 0 & \left(\bar{C}+\tilde{D}_{12}\Delta G_k\tilde{C}_2\right)^T\\
* & * & -\gamma I & \left(\bar{D}+\tilde{D}_{12}\Delta G_k\tilde{D}_{21}\right)^T\\
* & * & * & -\gamma I
\end{bmatrix}<0
\tag{21}
$$

The double homotopy process for searching a decentralized controller is described as below:

Step 1: Compute a centralized $\mathcal{H}_\infty$ controller G_C, as well as co-existing P_C and γ_C, and then separate $G_{C,diag}$ and $G_{C,off}$ according to Eq. (16a).

Step 2: Set the upper limit $K_{\max}$ for K, e.g. 2^{13}, and $\gamma_{\max}$ for γ, e.g. $2^8\gamma_C$. Initialize K, e.g. 2^6, $k\leftarrow 1$, $P_0\leftarrow P_C$, $G_0\leftarrow G_C$, $\gamma_0\leftarrow \gamma_C$.

Step 3: At step k, calculate the symmetric increment variable matrix ΔP_k, the structured increment variable matrix ΔG_k, and scale variable γ_k in the following LMI problem.

$$\begin{aligned} &\text{Minimize } \gamma_k \\ &\text{Subject to } V(\Delta G_k, \Delta P_k) < 0,\ P_{k-1} + \Delta P_k > 0,\ \|\Delta P_k\| < \lambda \|P_{k-1}\|,\ \|\Delta G_k\| < \lambda \|G_C\|,\ \gamma_k \geq \gamma_{k-1}. \end{aligned} \tag{22}$$

Step 4: Set $G_k \leftarrow G_{k-1} - \lambda G_{C,off} + \Delta G_k$ and $P_k \leftarrow P_{k-1} + \Delta P_k$. Check that the triplet (G_k, P_k, γ_k) satisfies the inequality Eq. (13). If they do, recalculate P_k by fixing G_k and γ_k in Eq. (13) to improve the condition number of P_k, and then go to Step 5. If not, set $K \leftarrow 2K$. If $K<K_{\max}$, repeat Step 3 with the initial value P_0, G_0, γ_0; otherwise set $\gamma_0 \leftarrow 2\gamma_C$ under the constraint $\gamma_0 \leqslant \gamma_{\max}$, and go to Step 3 with the initial value P_0, G_0, K, k. If γ_0 grows larger than the pre-set limit $\gamma_{\max}$, it is concluded that the algorithm does not converge.

Step 5: If $k = K$, the desired decentralized $\mathcal{H}_\infty$ controller is given by G_k. If not, set $k \leftarrow k+1$, and repeat Step 3 with the updated P_k, G_k, and γ_k.

It should be noted that this double homotopy method is heuristic and cannot guarantee convergence. Even if the process converges, the solution may still be a local optimum due to the non-convex nature of the decentralized control problem. On the other hand, non-convergence does not imply the non-existence of a decentralized $\mathcal{H}_\infty$ controller.

NUMERICAL EXAMPLE

This section studies performance comparison between the proposed decentralized controller design and centralized design, using a six-story model structure. The six-story structure is shown in Figure 2(a). Lumped mass parameters are provided in Figure 2(b) and other parameters are described in [12]. Three ideal actuators are installed on the 1st, 3rd and 5th floor, respectively. Through a V-brace, every actuator can apply control force between two neighboring floors.

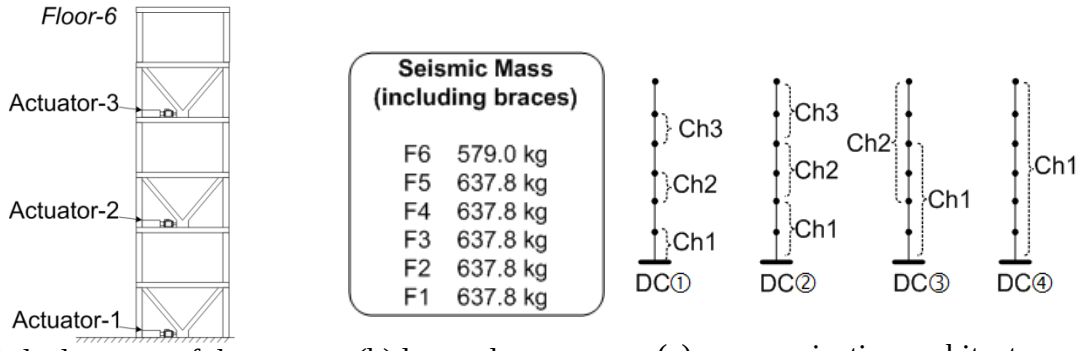

(a) deployment of three actuators (b) lumped masses of the structure (c) communication architecture for different DC

Figure 2. A six-story model structure centralization (DC)

The measurement output $m[k]$ are denoted as the inter-story drifts described in Eq. (23a). Sensor noise can influence the measurement results, and worsen the control performance. In this simulation, the sensor noise level is set as 0.1% of the sensor signal. Considering the time delay and sensor noise, the feedback signal $y[k]$ is formed as in Eq. (3). Eq. (23b) defines the response output $z[k]$ as the combination of inter-story drifts and control force with different weightings .

$$m[k]=\begin{bmatrix} q_1[k] & q_2[k]-q_1[k] & \cdots & q_6[k]-q_5[k] \end{bmatrix}^{\mathrm{T}} \tag{23a}$$

$$z[k]=\begin{bmatrix} \sqrt{10^4}\begin{pmatrix} q_1[k] & q_2[k]-q_1[k] & \cdots & q_6[k]-q_5[k] \end{pmatrix}, & \sqrt{10^{-9}}\begin{pmatrix} u_1 & u_2 & u_3 \end{pmatrix} \end{bmatrix}^{\mathrm{T}} \tag{23b}$$

As shown in Figure 2(c), four different feedback cases are studied, representing different degrees of centralization (DC). In each DC, there exist one or more communication subnets (as denoted by channels Ch1, Ch2, etc). A larger number of DC represents a higher level of centralization. For example, DC① means each subnet or channel covers only one story and there are three subnets totally. Each subnet in DC② covers two stories and a total of three subnets exist, without overlapping between two channels. For case DC③, each subnet covers four stories and the two communication channels overlap at 3rd and 4th stories. For DC④, only one subnet exists and covers all six stories, representing centralized control.

In practical implementation, the sampling period for different control architecture is determined by the network communication time and computation time of the embedded controllers. For a particular control system, values of the time delays can be measured according to sensor and controller deployment. As commonly encountered, the time delay in this study equals one sampling time step, i.e. the time delay equals one sampling period. Due to the least amount of communication and computation required, case DC① entails shortest sampling period and least time delay. A larger number of DC usually indicates more time is required for communication and computation. Case DC④ thus has the longest sampling period and time delay. Using a prototype wireless feedback control system as an example [17], the sampling period and time delay from DC① to DC④ adopted in this simulation are displayed in Table 1.

Table 1. Feedback time delay and sampling period for four different DCs (unit: ms)

DC①	DC②	DC③	DC④
15	20	25	52

The controllers for different DC cases are designed using the proposed double homotopy method for discrete time domain. The 1940 El Centro NS earthquake record is adopted as the ground excitation. The peak ground acceleration is scaled to 1 m/s^2. Classical Newmark integration is performed to compute time histories of structural response during the earthquake. For all cases with control and without control, the structure response is evaluated by peak inter-story drifts shown in Figure 3(a). Theoretically, the system should still be stable for all cases, even with ideal actuators that are capable of producing any desired forces. However, it is found that DC① and DC④

demonstrate unstable structural response in the Newmark integration, which means that the marginally low stability of these two cases is easily disturbed in the numerical integration. Figure 3(b) shows that due to instability, DC① and DC④ have prohibitively high requirements on actuator force. The low stability of DC① is likely because not enough measurement feedback is available, even though this case has the fastest response, i.e. least time delay. Meanwhile, the low stability of DC④ is due to its long time delay.

For the three stable cases (DC②, DC③, and without control), Figure 3(c) and Figure 3(d) illustrate peaks and RMS (root-mean-square) values of inter-story drifts. At the 2nd story, the structure without control has highest peak inter-story drift of 8×10^{-3}m and highest RMS inter-story drift of nearly 2.5×10^{-3}m. Both DC② and DC③ reduce peak and RMS of inter-story drifts, particularly for the 2nd story. In this example, DC③ performance is better than DC②, likely because DC③ has more measurement information available while not much longer time delay.

For DC② and DC③, the peak force and RMS force are shown in Figure 3(e) and Figure 3(f). Both cases required reasonable actuator capacities that can be generated in practice. Overall, it is observed that with reasonable time delay, the more measurement data available for each sub-controller, the better performance can be achieved in decentralized control.

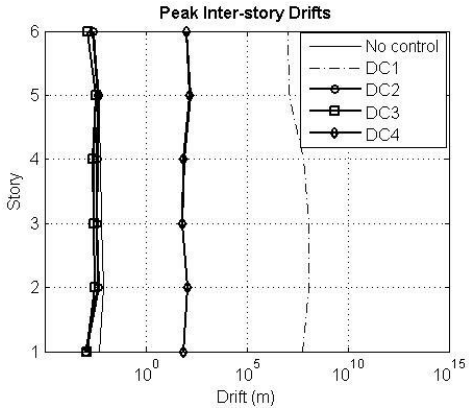

(a) peak inter-story drifts for all cases

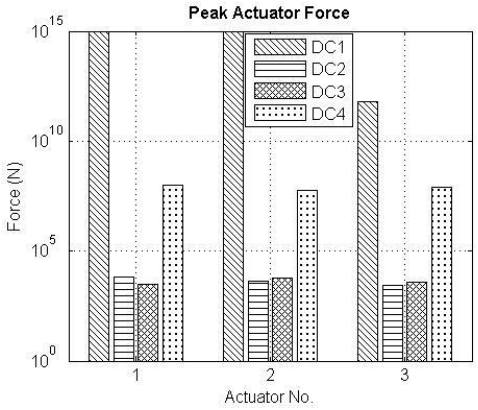

(b) peak actuator forces for all control cases

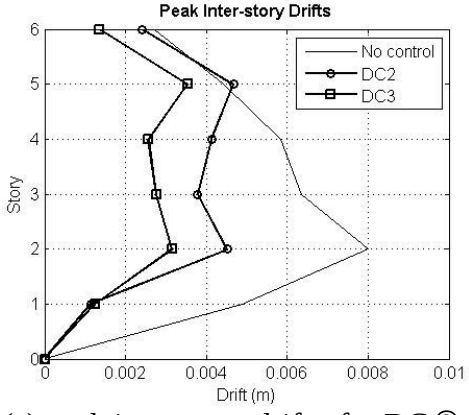

(c) peak inter-story drifts for DC②, DC③, and no control

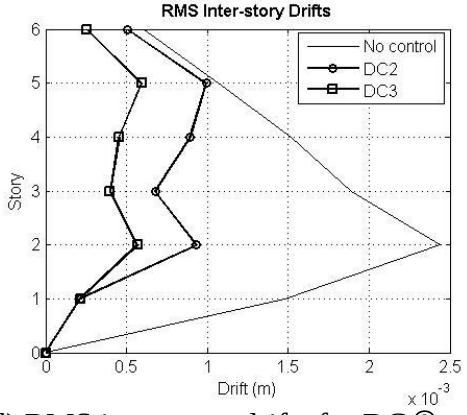

(d) RMS inter-story drifts for DC② and DC③

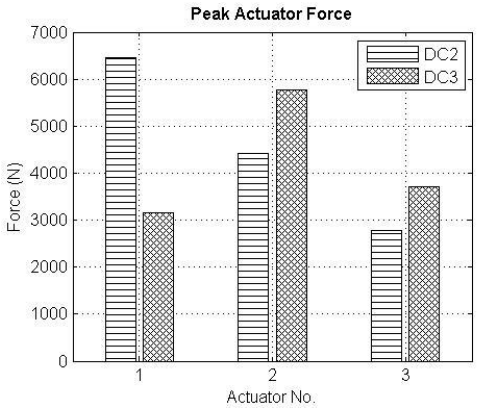

(e) peak actuator forces for DC② and DC③

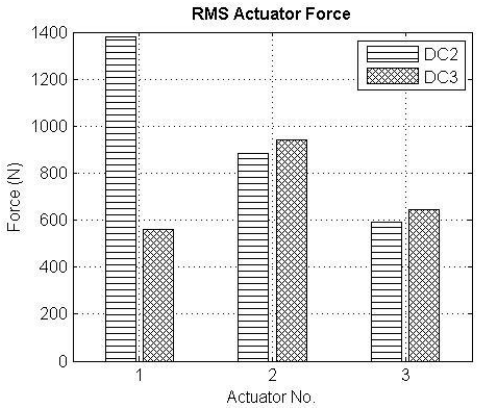

(f) RMS actuator forces for DC② and DC③

Figure 3. Simulation results for decentralized and centralized control with ideal actuators:

SHAKE TABLE EXPERIMENTS

To further study the decentralized $\mathcal{H}_\infty$ structural control, shake table experiments on a two-story frame with two active mass dampers (AMD) are conducted. The two-story frame model is obtained through Lagrange's method with the setup parameters. Decentralized $\mathcal{H}_\infty$ controllers are designed with time delay through the double homotopy approach, and tested in the shake table experiments.

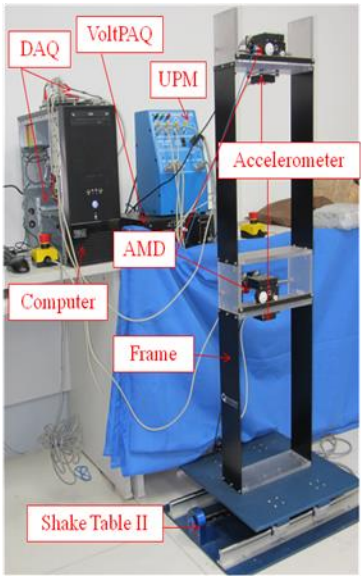

(a) photo of experimental setup

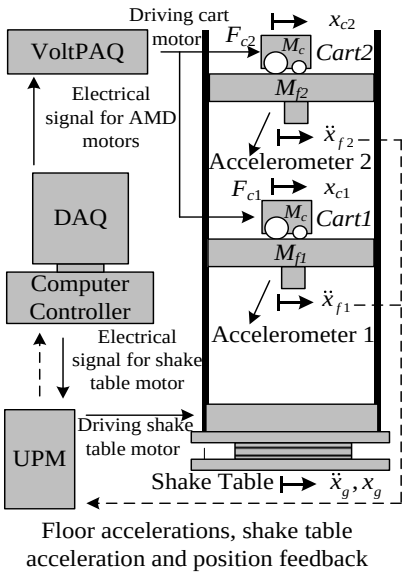

(b) diagram of experimental setup

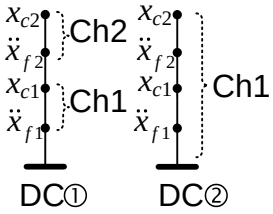

(c) communication architecture for different DC

Figure 4. Two-story frame with two AMDs

Experimental Setup

The experimental setup is made by Quanser Inc. The setup consists of a shake table, a Universal Power Module (UPM), a two-story frame with two AMDs, a VoltPAQ power amplifier for the AMDs, a data-acquisition (DAQ) card, and a PC running the QUARC control software. The QUARC software is integrated with MATLAB Simulink, and can be called inside a Simulink window.

As illustrated in Figure 4, according to input earthquake record, the computer calculates the current to drive the shake table, and then transmits the signals through DAQ to UPM. The DAQ is interface with other devices and collects data at 500Hz sampling frequency. UPM amplifies the current signals, and then drives the electric motor of the shake table. At each sampling step, the shake table sends its acceleration (detected by an accelerometer) and position (detected by an encoder) data back to DAQ through UPM. At the same time, the shake table movement excites the 2-story frame to vibrate. Each floor of the structure is equipped with a capacitive single-chip accelerometer with full scale range of $\pm 5\,\mathrm{g}$ and sensitivity of (9.81 m/s^2)/V. The AMD cart position on each floor is measured by an encoder with a high resolution of 4096 counts per revolution. The floor acceleration signals $\ddot{x}_{f1}$ and $\ddot{x}_{f2}$ are sent to DAQ through UPM. The position signals of the moving carts, x_{c1} and x_{c2}, are detected by AMD encoders and also collected by DAQ. Computer makes optimal control decision according to DAQ sampling data, and sends required voltage to VoltPAQ. VoltPAQ then drives the cart motors of AMDs to generate control force F_{c1} and F_{c2}. Through this feedback control loop, the structural response can be suppressed by the control forces.

Modeling and Control Strategies

Following the experimental setup, a dynamic model of the two-story frame with two-AMDs is obtained by Lagrange's method. The dynamic model can be transformed following Eq. (1). The vector q in Eq. (2) can be described as:

$$q = \begin{bmatrix} q_1 & q_2 & q_3 & q_4 \end{bmatrix}^{\mathrm{T}} = \begin{bmatrix} x_{c1} + x_{f1} - x_g & x_{f1} - x_g & x_{c2} + x_{f2} - x_g & x_{f2} - x_g \end{bmatrix}^{\mathrm{T}} \qquad (24)$$

As shown in Figure 4, x_{c1} (or x_{c2}) denotes the 1st (or 2nd) AMD cart displacement with respect to the 1st floor (or 2nd floor); x_{f1} (or x_{f2}) denotes the 1st (or 2nd) floor absolute displacement; x_g is the ground displacement. As a result, the four entries in Eq. (24) are the relative displacements of 1st AMD cart, 1st floor, 2nd AMD cart and 2nd floor (with respect to ground). The sensor measurement consists of two floor accelerations and two AMD cart positions, as defined in Eq. (25a). The structural response output contains the inter-story drift and weighted voltages for driving cart motors, as shown in Eq. (25b).

$$m[k] = \begin{bmatrix} x_{c1} & \ddot{x}_{f1} & x_{c2} & \ddot{x}_{f2} \end{bmatrix}^{\mathrm{T}} \qquad (25a)$$

$$z[k] = \begin{bmatrix} \left(x_{f1} - x_g \quad x_{f2} - x_{f1}\right), & \left(V_{m1} \quad V_{m2}\right) \times 4\mathrm{e}^{-2} \end{bmatrix}^{\mathrm{T}} \qquad (25b)$$

where V_{mi} is the voltage driving the i-th cart motor (i = 1, 2). As detailed in Quanser user manual, higher voltage V_{mi} for the cart motor generates larger force F_{ci}. Therefore, the control signal can be expressed by the cart voltage as $u = [V_{m1}, V_{m2}]^T$, instead of directly as the AMD forces.

All the sensors, including accelerometers and encoders, are connected with the DAQ card by cables. Because communication network is cabled for this small test structure, and all the controller computation is performed by a computer, the time delay is much shorter than using wireless communication and embedded computing by a microcontroller, as in [17]. In order to emulate longer time delay (which is more typical in practice with large structures) in the experiments, a rate transition block and a unit delay block are added into Simulink model as shown in Figure 5.

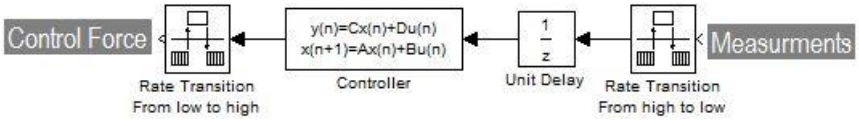

Figure 5. Simulink block diagram for sampling period changing and delay

As illustrated in Figure 5, the measurement data is sampled by the sensors at 2ms sampling period and is input into the high-to-low rate transition block, which can increase the sampling period from 2ms to 26ms. The unit delay block can delay by one sampling period before transferring measurement data to controller. The low-to-high rate transition block can reduce the sampling period from 26ms back to 2ms, so that the sampling period is uniform with the entire system. As a result, the control force calculated by controllers is held at the same value as zero-order hold during every 26ms. With the Simulink modules, the experiment with time-delayed control can be conducted.

Through double homotopy method, a decentralized $\mathcal{H}_\infty$ controller for case DC① in Figure 4(c) is designed. DC② is the centralized control case. El-Centro earthquake (Imperial Valley, Station 952, 10/15/79) record is employed with a scaled peak acceleration 0.519g (i.e. 5.09 m/s^2). Different time delays for case DC① and DC② is assumed to be 2ms and 26ms, respectively. Besides the two feedback control cases, another passive TMD (tuned mass damper) case is tested, where the two mass dampers are used to suppress structural response with zero input voltage V_{m1} and V_{m2} to AMD motors. The frame performances are compared between DC①, DC②, and TMD control cases in Figure 6.

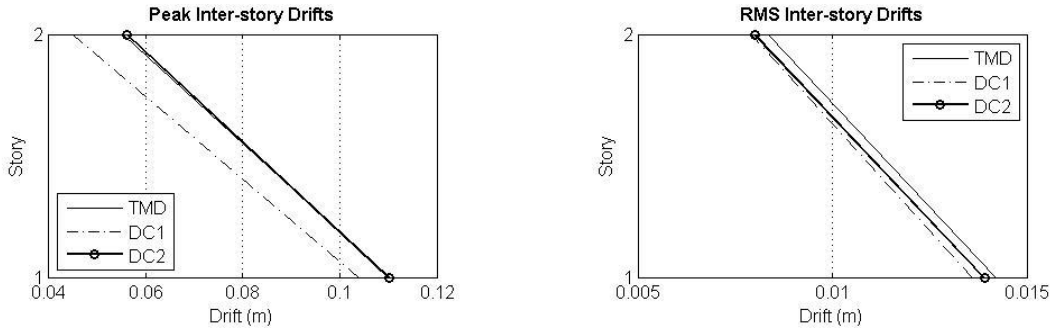

(a) peak inter-story drifts (b) RMS inter-story drifts

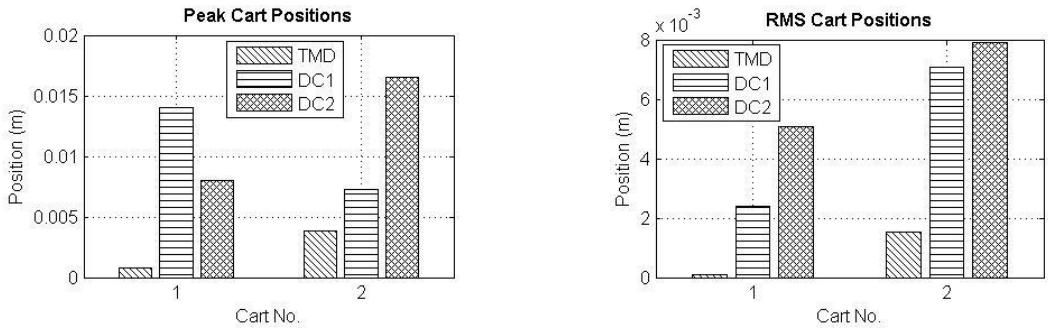

(c) peak cart positions (d) RMS cart positions

Figure 6. Experimental results for TMD, decentralized, and centralized control

In Figure 6(a) and (b), the peak inter-story drifts in 1st story and 2nd story for DC① are 1 cm less than TMD and DC②. DC② is the centralized control and does not perform better than passive TMD, due to the 26ms time delay. Cart position means the cart displacement with respect to the corresponding floor. The larger the cart displacement is, the larger the voltage input to cart motor is, which also means a higher requirement on control force. As shown in Figure 6(c) and (d), cart movements are the smallest in the passive TMD case without voltage control. DC① and DC② show larger cart displacements than TMD, and the cart displacements of DC② are much larger than DC①. This means due to the longer time delay, centralized DC② uses higher voltage and entails more control effort, but cannot suppress the response as well as decentralized DC①. Therefore, benefiting from less time delay required by a decentralized feedback system, decentralized control can perform better than the centralized scheme which usually has longer latency.

SUMMARY AND CONCLUSION

This paper presents a decentralized $\mathcal{H}_\infty$ controller design in discrete time domain. Considering time delay, the decentralized $\mathcal{H}_\infty$ controller minimizes the $\mathcal{H}_\infty$ norm of the closed-loop system. According to the bounded real lemma, the controller design requires solving a bilinear matrix inequality (BMI) problem, which is NP-hard and cannot be solved using projection lemma due to the block-diagonal pattern constraint to controllers. A double homotopy method is employed to approximate this BMI problem to a series of linear matrix inequality (LMI) problems, which gradually deforms the centralized controller to a decentralized controller.

The control performance of the decentralized $\mathcal{H}_\infty$ controller is first validated through a six-story numerical example. It shows that for cases with acceptable time delay (e.g. DC② and DC③), the more measurement data is available for decentralized sub-controllers, the better the control performance is. When the time delay is too long (DC④) or not enough measurement data (DC①) is available for the sub-controllers, the feedback system has poor stability. This conclusion is also corroborated by shake table experiments using a two-story frame with two AMDs. Longer time delay can worsen the performance of the controller. Due to less time delay, decentralized controller DC① achieves better performance than the centralized controller DC② in experiments.

Because the proposed double homotopy method is heuristic, significant amount of future studies are needed to compare its performance with other existing methods for decentralized control design.

ACKNOWLEDGEMENT

The authors are grateful for the support National Natural Science Foundation of China (grant number 51121005 and 50708016) and National Earthquake Special Founding of China (grant number 200808074), and also appreciate the experiment device supported by Structural Health Monitoring and Control Lab in Faculty of Infrastructure Engineering, Dalian University of Technology. Dr. Yang Wang is supported by the U.S. National Science Foundation CAREER Award CMMI-1150700. Any opinions, findings, and conclusions or recommendations expressed in this publication are those of the authors and do not necessarily reflect the view of the sponsors. In addition, The authors would like to thank Prof. Chin-Hsiung Loh and Dr. Kung-Chun Lu of the National Taiwan University, as well as Dr. Pei-Yang Lin of NCREE, for generously providing the numerical model of the six-story example structure.

REFERENCES

1. Adeli H. Wavelet-Hybrid Feedback-Least Mean Square Algorithm for Robust Control of Structures. *Journal of Structural Engineering* 2004; **130**(1):128-137.
2. Kim Y., Hurlebaus S.,Langari R. Model-Based Multi-input, Multi-output Supervisory Semi-active Nonlinear Fuzzy Controller. *Computer-Aided Civil and Infrastructure Engineering* 2010; **25**(5):387-393.
3. Lin C. C., Chen C. L.,Wang J. F. Vibration Control of Structures with Initially Accelerated Passive Tuned Mass Dampers under Near-Fault Earthquake Excitation. *Computer-Aided Civil and Infrastructure Engineering* 2010; **25**(1):69-75.
4. Spencer B. F., Jr.,Nagarajaiah S. State of the Art of Structural Control. *Journal of Structural Engineering* 2003; **129**(7):845-856.
5. Sandell N., Jr., Varaiya P., Athans M.,Safonov M. Survey of decentralized control methods for large scale systems. *Automatic Control, IEEE Transactions on* 1978; **23**(2):108-128.
6. Siljak D. D. *Decentralized Control of Complex Systems*. Academic Press: Boston, 1991.
7. Siljak D. D. Decentralizedcontrol and computations: status and prospects. *Annual Reviews in Control* 1996; **20**:131-141.
8. Lynch J. P.,Law K. H. Decentralized control techniques for large scale civil structural systems. *Proceedings of the 20th International Modal Analysis Conference*, Los Angeles, CA, 2002.
9. Xu B., Wu Z. S.,Yokoyama K. Neural networks for decentralized control of cable-stayed bridge. *Journal of Bridge Engineering* 2003; **8**(4):229-236.
10. Swartz R. A.,Lynch J. P. Redundant Kalman Estimation for a Distributed Wireless Structural Control System. *Proceedings of the US-Korea Workshop on Smart Structures Technology for Steel Structures*, Seoul, Korea, 2006.
11. Rofooei F. R.,Monajemi-Nezhad S. Decentralized control of tall buildings. *The Structural Design of Tall and Special Buildings* 2006; **15**(2):153-170.
12. Lu K. C., Loh C. H., Yang J. N.,Lin P. Y. Decentralized sliding mode control of a building using MR dampers. *Smart Materials and Structures* 2008; **17**(5):055006.
13. Ma T. W., Xu N. S.,Tang Y. Decentralized robust control of building structures under seismic excitations. *Earthquake Engineering & Structural Dynamics* 2008; **37**(1):121-140.

14. Loh C. H.,Chang C. M. Application of centralized and decentralized control to building structure: analytical study. *Journal of Engineering Mechanics* 2008; **134**(11):970-982.
15. Wang Y., Law K. H.,Lall S. Time-delayed decentralized H_∞ controller design for civil structures: a homotopy method through linear matrix inequalities. *Proceedings of the 2009 American Control Conference (ACC 2009)*, St. Louis, MO, USA, 2009.
16. Wang Y. Time-delayed dynamic output feedback H_∞ controller design for civil structures: a decentralized approach through homotopic transformation. *Structural Control and Health Monitoring* 2011; **18**(2):121-139.
17. Wang Y., Swartz R. A., Lynch J. P., Law K. H., Lu K.-C.,Loh C.-H. Decentralized civil structural control using real-time wireless sensing and embedded computing. *Smart Structures and Systems* 2007; **3**(3):321-340.
18. Gahinet P.,Apkarian P. A linear matrix inequality approach to H_∞ control. *International Journal of Robust and Nonlinear Control* 1994; **4**(4):421-448.
19. VanAntwerp J. G.,Braatz R. D. A tutorial on linear and bilinear matrix inequalities. *Journal of Process Control* 2000; **10**(4):363-385.
20. Kocvara M.,Stingl M. PENNON - A Code for Convex Nonlinear and Semidenite Programming. *Optimization Methods and Software* 2003; **18**(3):317-333.
21. Mehendale C. S.,Grigoriadis K. M. A double homotopy method for decentralised control design. *International Journal of Control* 2008; **81**(10):1600 - 1608.